

Jun Wang
Sachin Velankar

Strain recovery of model immiscible blends without compatibilizer

Received: 7 January 2005
Accepted: 25 August 2005
Published online: 7 October 2005
© Springer-Verlag 2005

J. Wang · S. Velankar (✉)
Department of Chemical Engineering,
University of Pittsburgh,
Pittsburgh, PA, USA
E-mail: velankar@pitt.edu

Abstract Strain recovery after the cessation of shear was studied in model immiscible blends composed of polyisobutylene drops (10–30% by weight) in a polydimethylsiloxane matrix. Blends of viscosity ratio (viscosity of the drops relative to the matrix viscosity) ranging from 0.3 to 1.7 were studied. Most of the strain recovery was attributable to interfacial tension, and could be well-described by just two parameters: the ultimate recovery and a single retardation time. Both these parameters were found to increase with the capillary number of the drops prior

to cessation of shear. For blends that had reached steady shear conditions, the ultimate recovery decreased with increasing viscosity ratio, whereas the retardation time increased with increasing viscosity ratio. The retardation time was well-predicted, but the ultimate recovery was over-predicted by a linear viscoelastic model developed previously by Vinckier et al. (Rheol Acta 38:65–72, 1999).

Keywords Immiscible blends · Creep recovery · Drop deformation · Rheology · Interfacial tension

Introduction

The rheological properties of blends of immiscible homopolymers have received much attention in recent years (Tucker and Moldenaers 2002). Several publications have been devoted to examining the relationship between the rheology and morphology of two-phase blends. A key strategy employed by many researchers was to conduct experiments on “model” blends that were comprised of rheologically-simple polymers. This gave the enormous advantage that any non-Newtonian behavior of the blend could be ascribed unambiguously to interfacial effects, and thus correlated quantitatively with the morphology of the blend.

We are presently studying the effects of added compatibilizer on the rheology of such model immiscible blends. As a part of this research we conducted several “baseline” measurements on blends without compatibilizer, some of which are of interest in their own right. Here we summarize some observations of the creep

recovery after cessation of shear of model uncompatibilized blends with droplet-matrix morphologies. These results add significantly to the data on creep recovery of immiscible blends, in particular, we are unaware of any previous publications that detail the effects of volume fraction and viscosity ratio of the immiscible phases on the creep recovery. The effects of added compatibilizer are discussed in the accompanying paper.

Theory

When under shear, droplets in the blend are deformed and partially oriented along the flow direction. Upon cessation of shear, these droplets retract back to their spherical shape. This retraction drives strain recovery of the blend (Gramespacher and Meissner 1992, 1995; Vinckier et al. 1999); clearly if the drops are highly deformed and oriented prior to cessation of shear, a larger recovery is expected. Such interface-driven recovery

adds to any recovery from the bulk phases themselves. Since the blends discussed here are composed of nearly Newtonian bulk phases, the recovery is almost entirely due to the interface.

Vinckier et al. (1999) developed a model for the creep recovery of blends from steady shear in the linear viscoelastic regime and we will summarize their main results here. The linear viscoelastic properties of immiscible blends of Newtonian components can be described by a Jeffreys model (Oldroyd 1953; Vinckier et al. 1999)

$$\left(1 + \lambda_{F1} \frac{d}{dt}\right) \sigma = \eta_b \left(1 + \lambda_{F2} \frac{d}{dt}\right) \dot{\gamma} \quad (1)$$

where σ and γ are the shear stress and shear strain respectively, and an overdot denotes a time derivative. The above equation describes the blend in terms of three properties: the blend viscosity, η_b , the relaxation time, λ_{F1} , and the retardation time, λ_{F2} . The subscript ‘‘F’’ is intended to denote the ‘‘form’’ relaxation or retardation processes attributable to retraction of deformed drops back to a spherical drop shape (Jacobs et al. 1999); in the following paper, additional processes will be introduced. Integrating this equation with initial conditions corresponding to cessation of a steady shear stress, Vinckier et al. (1999) showed that the recovery follows exponential kinetics:

$$\gamma = \gamma_\infty [1 - \exp(-t/\lambda_{F2})] \quad (2)$$

where

$$\gamma_\infty = \frac{\sigma_0}{\eta_b} (\lambda_{F1} - \lambda_{F2}) \quad (3)$$

where σ_0 is the shear stress prior to recovery and γ_∞ is the ultimate recovery. Substituting $\sigma_0 = \eta_b \dot{\gamma}_0$, where $\dot{\gamma}_0$ is the shear rate during the steady shearing prior to recovery, Eq. 3 becomes

$$\gamma_\infty = \dot{\gamma}_0 (\lambda_{F1} - \lambda_{F2}) = \lambda_{F1}^* - \lambda_{F2}^* \quad (4)$$

where $\lambda_{F1}^* = \dot{\gamma}_0 \lambda_{F1}$ and $\lambda_{F2}^* = \dot{\gamma}_0 \lambda_{F2}$ are the dimensionless relaxation and retardation times respectively. Vinckier et al. used the following expressions for λ_{F1}^* and λ_{F2}^* given by Graebling et al. (1993b):

$$\lambda_{F1}^* = \text{Ca} \frac{19p + 16}{4} \left[\frac{2p + 3 - 2\phi(p-1)}{10(p+1) - 2\phi(5p+2)} \right] \quad (5)$$

$$\lambda_{F2}^* = \text{Ca} \frac{19p + 16}{4} \left[\frac{2p + 3 + 3\phi(p-1)}{10(p+1) + 3\phi(5p+2)} \right] \quad (6)$$

where the capillary number, Ca, of the drops is defined as

$$\text{Ca} = \frac{R\eta_m \dot{\gamma}_0}{\alpha} \quad (7)$$

Here R is the drop radius, η_m is the matrix viscosity and α is the interfacial tension.

In this paper, only terms up to order ϕ will be retained. Therefore, Eqs. 5 and 6 are expanded in powers of ϕ :

$$\lambda_{F1}^* = \text{Ca} \frac{19p + 16}{40(p+1)} \left[2p + 3 + \frac{19p + 16}{5(p+1)} \phi + \text{O}(\phi^2) \right] \quad (8)$$

$$\lambda_{F2}^* = \text{Ca} \frac{19p + 16}{40(p+1)} \left[2p + 3 - \frac{3(19p + 16)}{10(p+1)} \phi + \text{O}(\phi^2) \right] \quad (9)$$

Eqs. 8 and 9 are identical to those provided by Oldroyd (1953). Substituting Eqs. 8 and 9 into Eq. 4:

$$\gamma_\infty = \text{Ca} \frac{1}{80} \left(\frac{19p + 16}{p+1} \right)^2 [\phi - \text{O}(\phi^2)] \quad (10)$$

Equation 10 helps make the connection between drop deformation and creep recovery explicit. Specifically, Taylor’s theory (Taylor 1934) predicts that at small Ca, the deformation of the drops is given by

$$D_{\text{Taylor}} = \text{Ca} \frac{19p + 16}{16(p+1)} \quad (11)$$

Substituting into Eq. 10,

$$\gamma_\infty = D_{\text{Taylor}} \frac{1}{5} \left(\frac{19p + 16}{p+1} \right) [\phi - \text{O}(\phi^2)]. \quad (12)$$

The linear viscoelastic theory thus predicts that the ultimate recovery proportional to the deformation.

In summary, the Vinckier model suggests that the recovery process can be captured in terms of only two parameters, the ultimate recovery and the dimensionless retardation time, both of which are proportional to the Ca prior to cessation of shear. Other noteworthy features of the linear viscoelastic theory of Vinckier et al. (1999) are: The absolute value of drop size or interfacial tension does not appear in any of the above equations: the dimensionless rheological properties γ_∞ and λ_{F2}^* can be expressed in terms of the dimensionless parameters Ca, p , and ϕ . The ultimate recovery from Eq. 10 is only weakly dependent on p . This is related to the weak dependence of D_{Taylor} on p (Eq. 11) as pointed out by Taylor. The coefficient of ϕ^2 in Eq. 10 is negative; the ultimate recovery is predicted to increase slower than the volume fraction due to pairwise drop interactions, provided Ca is held constant. The coefficient of ϕ in Eq. 9 is also negative; the dimensionless retardation time reduces as the volume fraction of the drops increases, provided Ca is held constant.

It must be emphasized that Eqs. 9 and 10 have a strong dependence on Ca. Therefore verifying the last

two features (trends of γ_∞ and λ_{F2}^* as ϕ increases) requires that Ca be held constant. This is difficult to do experimentally unless coalescence is very slow.

Experimental

Blends were composed of polyisobutylene (PIB) as the drop phase and polydimethylsiloxane (PDMS) as the matrix phase. Blends with 10, 20 and 30% by weight of PIB were studied. These correspond to volume fractions of 0.11, 0.21 and 0.32 respectively. The viscosities of the two components at the three temperatures of experiment are listed in Table 1. Both fluids were nearly-Newtonian under experimental conditions. Blends were prepared by mechanical mixing with a spatula as described previously, and degassed in a vacuum. Experiments were conducted in a TA Instruments AR2000 stress controlled rheometer in a 40 mm/1° cone angle using a Peltier cell to maintain sample temperature at the values listed in Table 1. The shear history of the samples is shown in Fig. 1a: samples were presheared at 480 Pa for 3,000 strain units, and the recovery was measured. Shearing was then continued at 120 Pa. The 120 Pa shearing was interrupted periodically to measure the recovery. For samples with 10 wt% drops, dynamic oscillatory experiments at 25% strain were also conducted subsequent to recovery. At this low weight percentage of drops, there was no change in the morphology of the sample over the timescale of a frequency sweep test.

No compatibilizer was added to any of the blends in this paper; compatibilizer effects are discussed in the accompanying paper.

Results

Experimental results of recovery

Figure 1b shows the creep recovery of blends with 10 and 30 wt% drops after shearing at 120 Pa for the various times specified in the figures. The recovery of the matrix phase PDMS is also plotted for comparison (the recovery of the PIB was too small to be measured). It is clear that the blends show significantly more

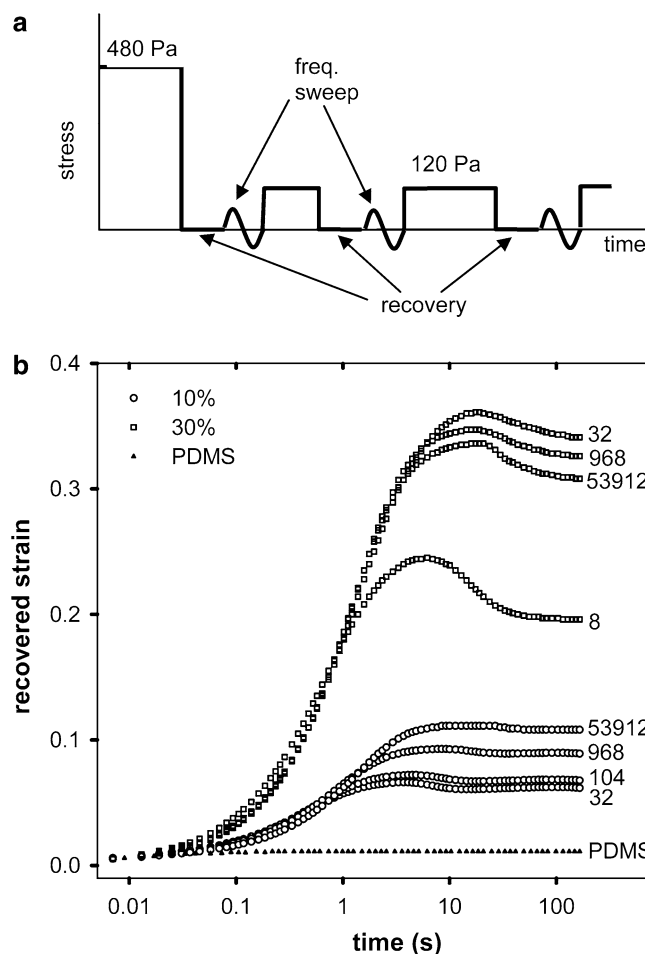


Fig. 1 **a** Schematic of shear history of samples. **b** Recovery of blends with viscosity ratio 1.1 and 10 wt% or 30 wt% drops at various times after stepping down the shear stress to 120 Pa.s. These times, in seconds, are listed alongside each curve

recovery than the components. While the ultimate recovery and the time to complete the recovery process vary with the volume fraction and viscosity ratio of the drops, the shape of the curves are qualitatively similar for all blends. The recovery curves are also qualitatively similar to the results of Vinckier et al. (1999) for a similar blend with 10 wt% drops. For the blends with 10 wt% drops, the ultimate recovery and the time required to complete the recovery process both increase with increasing shearing time. This can be understood easily: after reducing the shear stress from 480 to 120 Pa, initially-small drops grow by coalescence and are more deformed, and hence show more recovery. In contrast, for the blends with 30 wt% drops, the ultimate recovery is maximum at some short shearing time, and then reduces to its steady state value. The same was observed for the other two viscosity ratios (not shown). This result is not consistent with a monotonic increase in drop size and we have no explanation for it.

Table 1 Viscosities of components and viscosity ratios of blends

Pure components	Viscosity at 120 Pa shear stress Pa.s		
	17 °C	23 °C	32 °C
PIB	181	101	46
PDMS	106	94	159
Viscosity ratio p	1.70	1.10	0.29

A second notable feature, a reversal of recovery is evident for the blends in Fig. 1. Reversal is largest at short shearing times, especially for the blend with 30 wt% drops, but quite modest at steady state. Vincikier et al. (1999) claimed that they did not observe reversal of recovery in similar blends with 10 wt% drops, yet, weak reversal is evident in their own data (see Fig. 3 in Vincikier et al. 1999). Far stronger reversal of recovery in two-phase blends was first documented by Gramespacher and Meissner (1995), with up to a third of the maximum recovery being reversed. To our knowledge, a clear explanation of the reasons for reversal of recovery has not yet been established. Yet, since the components of the blends studied here show negligible recovery, one of the proposed explanations (Gramespacher and Meissner 1995), viz., a coupling between recovery from the bulk and recovery due to interfacial tension, can be ruled out. Reversal of recovery is not discussed further in this paper.

Data analysis

Figure 2 replots the data for both volume fractions after shearing for very long times (i.e. to steady state; see below) on a log-log scale. It is evident that much of the recovery occurring prior to 0.1 s is attributable to recovery of the matrix phase PDMS. Since we are primarily interested in the recovery that is attributable to the interface, this ‘‘component contribution’’ must be subtracted from the blend recovery. Following Vincikier et al. (1999), we do this in a simple-minded fashion. The quantity of interest, viz., the interfacial contribution to the recovery, $\gamma_{\text{interface}}(t)$ is obtained by simply subtracting the volume average contribution of the components:

$$\begin{aligned} \gamma_{\text{interface}}(t) &= \gamma_{\text{measured}}(t) - \sum \phi_i \gamma_i(t) \\ &\approx \gamma_{\text{measured}}(t) - \phi_{\text{PDMS}} \gamma_{\text{PDMS}}(t) \end{aligned} \quad (13)$$

where the second part of this expression is justified by the fact that the PIB phase shows negligible recovery. While this equation is not rigorous, the errors involved are expected to be small due to the nearly Newtonian nature of the pure components. After subtraction of the component contribution, the remaining recovery, which is attributable to interfacial tension, appears to be of a very simple nature. Indeed in accord with Vincikier et al. (1999), the single exponential kinetics of Eq. 2 appear to fit the recovery reasonably well (except the slight reversal of recovery, which obviously cannot be captured by any monotonically decaying function). The fits then yield the retardation time λ_{F2} , which can be made dimensionless by multiplying by the shear rate prior to the cessation of shear, thus obtaining λ_{F2}^* . To summarize, only two parameters of the recovery curves will be reported henceforth: the ultimate recovery γ_{∞} which is obtained

directly from the recovery curves, and the dimensionless retardation time λ_{F2}^* obtained from single-exponential fits. Both γ_{∞} and λ_{F2}^* refer to the interfacial contribution to the recovery as defined by Eq. 13.

For the blends with 10% of the dispersed phase, we also conducted dynamic oscillatory measurements immediately following the recovery; at the higher volume fractions, rapid quiescent coalescence did not permit obtaining the dynamic mechanical properties. A typical example of the dynamic moduli is shown in Fig. 6 in the Appendix. The characteristic relaxation time of the blend was calculated from storage modulus G' of the blends as described in the Appendix. The capillary number was calculated from this relaxation time by applying Eq. 9. Thus, the Ca of the blends immediately prior to recovery can be obtained from the dynamic oscillatory measurements, assuming that drops do not break during recovery. Due to some ambiguities in the fitting procedure, these values of Ca are expected to have systematic errors of about 10% i.e. all the Ca values of a particular blend could be varied by up to about 10% with minimal changes to the fitting quality.

Discussion

Figure 3a and b show the two parameters of the recovery γ_{∞} , and λ_{F2}^* for blends with 10 and 30 wt% drops. It is clear that both quantities show similar

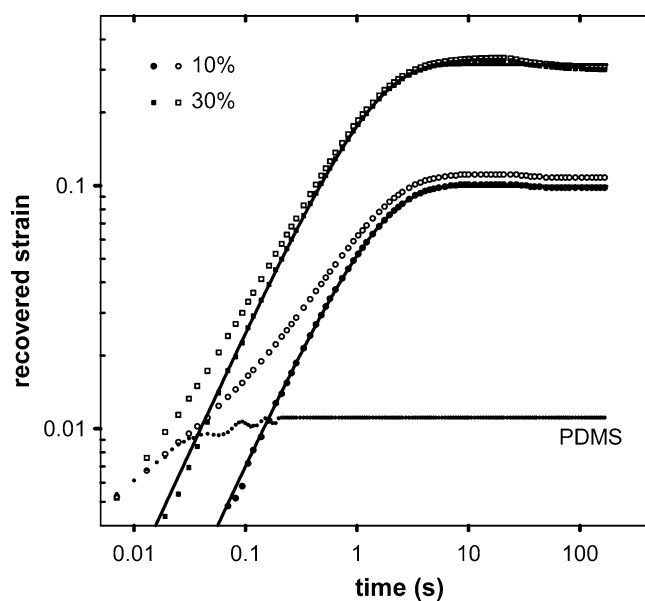
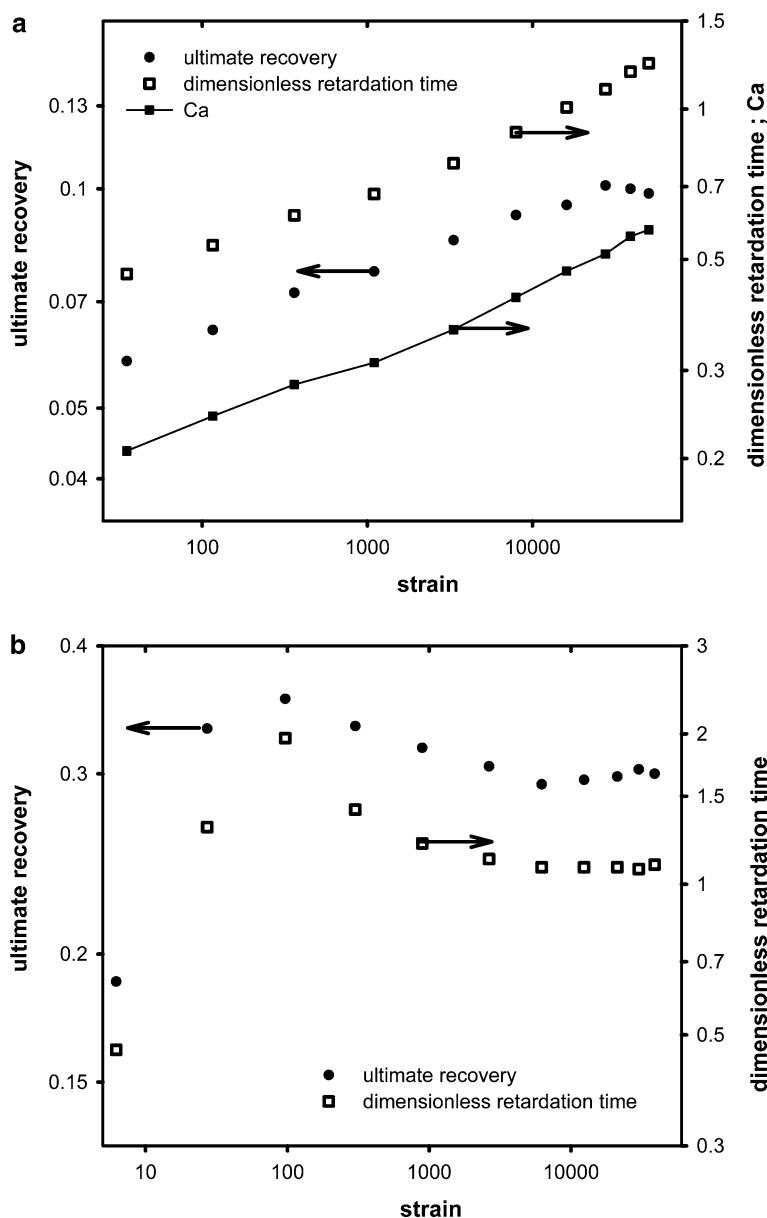


Fig. 2 Data analysis of recovery curves: Open symbols: ‘‘raw’’ recovery data; these are the same data labeled ‘‘53912’’ in Fig. 1. Filled symbols: recovery after subtraction of component contribution as per Eq. 11. Solid lines fits to single exponential kinetics Eq. 2

Fig. 3 Ultimate recovery and dimensionless retardation time for blends with viscosity ratio 1.1 and **a** 10% drops, and **b** 30% drops. All axes in both plots are logarithmic. The retardation time and the Ca for the blend in **(a)** did not reach steady state even after 15 h of shearing



trends. The maximum in ultimate recovery at very short shearing times mentioned in Sect. 4.1 is clearly evident in Fig. 3b. Figure 3a also plots the Ca values obtained from the dynamic mechanical experiments; evidently Ca and the dimensionless retardation time show exactly the same trend.

The data of Fig. 3a are replotted in Fig. 4 and compared with the predictions of Eqs. 9 and 10. Above it was mentioned that there is up to 10% systematic error in the Ca values; thus, the entire set of points corresponding to a particular viscosity ratio could be moved to the right or left by up to 10%. Considering this error, Eq. 9 seems to predict the retardation time reasonably well, however, Eq. 10 significantly overpredicts the

ultimate recovery. This comment requires immediate qualification. The Ca was obtained here from the relaxation time in dynamic oscillatory experiments, thus, Fig. 4a is essentially a plot of γ_∞ versus the relaxation time, and Fig. 4b is a plot of the retardation time versus the relaxation time. Thus, a more precise conclusion is that the Vinckier model is able to capture the ratio of the relaxation time to the retardation time accurately, but the γ_∞ resulting from this model is too large. This conclusion that γ_∞ is overpredicted is supported by results for blends with 20% or 30 wt% drops. For these blends, Ca values could not be obtained hence the predictions of Eqs. 9 and 10 cannot be tested directly. Yet, the ratio of γ_∞ and λ_{F2}^* can be compared with that predicted by the

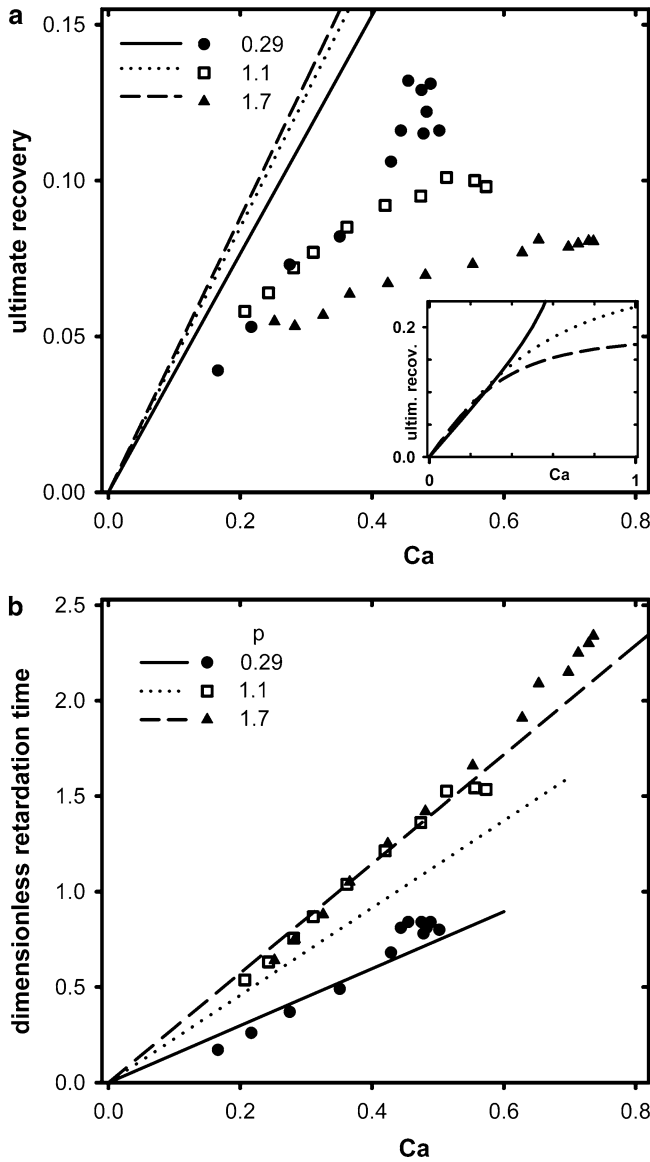


Fig. 4 **a** Ultimate recovery, and **b** dimensionless retardation time of blends with 10 wt% drops and various viscosity ratios. Lines represent Eq. 10 in (a), and Eq. 9 in (b). Inset to **a** is discussed in the text

Vinckier model. The experimental ratio $\gamma_\infty/\lambda_{F2}^*$ was found to be less than half that predicted by Eqs. 9 and 10, thus confirming that the ultimate recovery is indeed strongly over-predicted by the Vinckier model. Including terms with higher order in ϕ Eqs. 9 and 10 do not change this conclusion. In contrast Vinckier et al. (1999) concluded that Eq. 10 worked well for one specific blend ($p=0.44$, 10 wt% drops). It must be emphasized however that they obtained the Ca by a completely different method: microscopic measurements of drop size and independent measurements of interfacial tension were used calculate Ca from its definition (Eq. 7).

A second observation from Fig. 4a is that while the theory predicts a weak increase in the ultimate recovery with viscosity ratio (Eq. 10), the data show that γ_∞ decreases strongly with increasing viscosity ratio. This is probably due to fact that the linear viscoelastic theory assumes slightly deformed drops and hence is valid at only small Ca .

Lastly, the γ_∞ versus Ca curves seem to show qualitatively different shapes at different viscosity ratios: for $p=1.1$ or 1.7, the curves are slightly convex-up and γ_∞ appears to level off at high Ca , whereas for $p=0.29$, the curve is slightly convex-down and γ_∞ appears to increase sharply above $Ca=0.4$. We propose that this is directly related to the trends in drop deformation as Ca increases beyond the limit of Taylor's linear theory (Taylor 1934). Indeed Maffettone and Minale (1998) have proposed a model of drop deformation to capture such non-linear deformation behavior of drops. For simple shear flow, the Maffettone–Minale model gives

$$D_{MM} = \frac{\sqrt{f_1^2 + Ca^2} - \sqrt{f_1^2 + Ca^2 - f_2^2 Ca^2}}{f_2 Ca} \quad (14)$$

where f_1 and f_2 are functions of p and can also be functions of Ca . Note that Eq. 14 corrects a typographical error in the original paper. Maffettone and Minale (1998) recommended

$$f_1 = \frac{40(p+1)}{(2p+3)(19p+16)}. \quad (15)$$

Two choices were provided for f_2 . We will use

$$f_2 = \frac{5}{2p+3} \quad (16)$$

Substituting Eq. 14 instead of D_{Taylor} into Eq. 12, the inset of Fig. 4a is obtained. Clearly, the Maffettone–Minale model can qualitatively capture the convex-up vs convex-down trends of the γ_∞ versus Ca curves at various viscosity ratios, however, the ultimate recovery is still overpredicted. Using the alternative choice for f_2 (Maffettone and Minale 1998) does not improve agreement with the experimentally measured γ_∞ .

Finally, we examine the dependence of γ_∞ and λ_{F2}^* after cessation of steady shear on the volume fraction. Figure 5a shows that the ultimate recovery is either proportional to ϕ (at $p=1.1$) or increases faster than ϕ ($p=0.29$ or 1.7). At first glance this seems to contradict Eq. 10 in which the coefficient of ϕ^2 is negative. However, since the steady shear Ca is itself expected to increase with ϕ due to accelerated coalescence, a straightforward comparison with Eq. 10 is not possible. Figure 5b shows that the retardation time of the blends decreases significantly with increasing ϕ for blends with $p > 1$, but increases slightly for $p=0.29$. Once again,

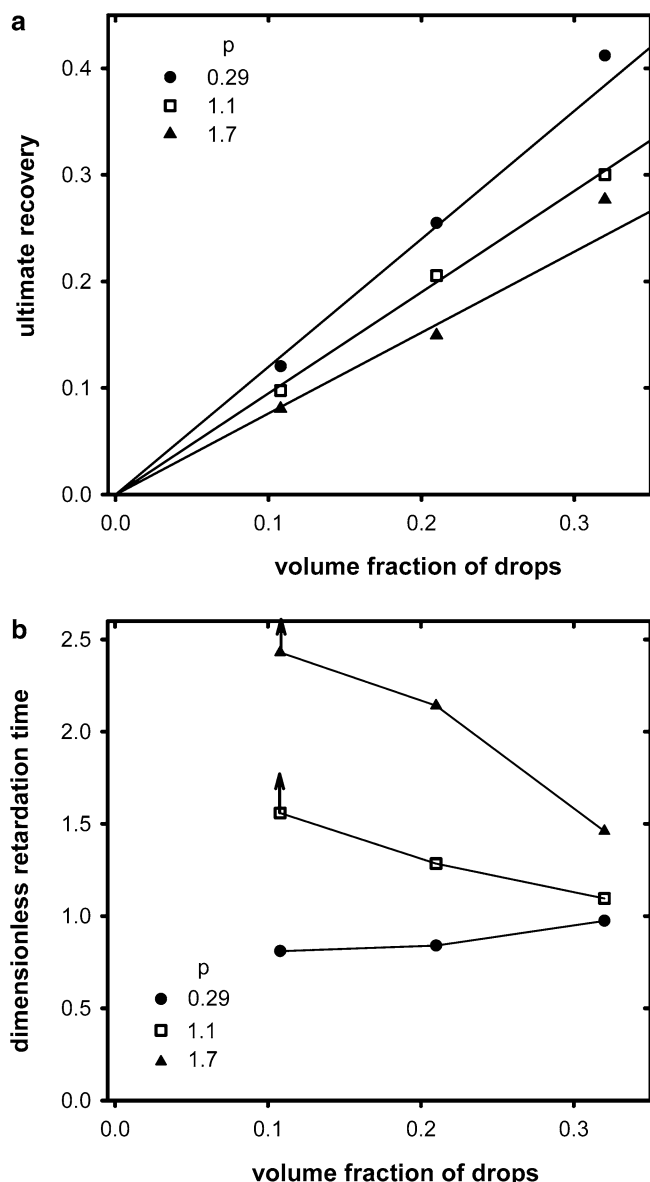


Fig. 5 Dependence of **a** ultimate recovery, and **b** dimensionless retardation time, after cessation of steady shear at 120 Pa on volume fraction of the dispersed phase at various viscosity ratios. In **a**, straight lines are only guides to the eye. The two vertical arrows for the 10% blends in **b** indicate that these retardation times were still increasing slowly with applied strain at the end of the experiment (although the γ_{∞} had reached a steady value)

direct comparisons with Eq. 9 are not possible due to the likely changes in the steady state Ca with viscosity ratio.

Summary and conclusions

Creep recovery of blends of immiscible, nearly Newtonian, polymer melts was studied, with the drop weight fraction ranging from 0.1 to 0.3 and the ratio of the viscosity of the drops to the matrix ranging from 0.3 to

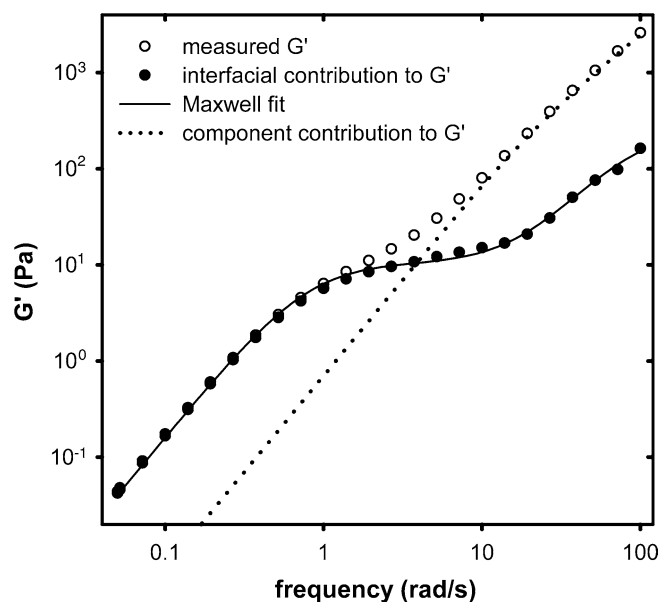


Fig. 6 Analysis of dynamic mechanical data. Open circles are the measured G' of a blend with 10 wt% drops, $p=1.1$, sheared for 53912 s at 120 Pa. The solid line corresponds to Eq. 17 with $n=2$ i.e. a sum of two Maxwell modes

1.7. The creep recovery attributable to the interface can be characterized by only two parameters: a single retardation time and the ultimate recovery.

For recovery after reaching steady state shearing conditions, the ultimate recovery steadily increased with increasing weight fraction of the drops and with decreasing viscosity ratio. The dimensionless retardation time showed the opposite trend generally increasing with decreasing weight fraction of drops and with increasing viscosity ratio.

For recovery before reaching steady shear conditions, Vinckier's model (1999) for creep recovery in the linear viscoelastic regime of emulsions was evaluated. The model was found to predict the retardation time well, but was also found to overpredict the ultimate recovery significantly. We conclude that the linear viscoelastic model of blend rheology can capture recovery qualitatively but not quantitatively.

Acknowledgements We are grateful to the University of Pittsburgh and the ACS Petroleum Research Fund (Grant #39931-G9) for supporting this research.

Appendix

Figure 6 shows a typical dynamic mechanical frequency sweep measurement for a blend with 10 wt% drops. Also shown is the G' expected from the components (calculated using the Palierne model with the interfacial

tension set to zero). The most obvious feature is the pronounced shoulder in the measured G' of the blend that is entirely absent from the components. This shoulder has been attributed to the interfacial tension and its characteristics can be related to the size of the drops in the blends (Graebling et al. 1993a, 1994; Vinckier et al. 1996). Such frequency sweep data have been analyzed extensively in past publications (Graebling et al. 1993a, 1994; Vinckier et al. 1996; Kitade et al. 1997; Velankar et al. 2001). Here we will follow the analysis outlined by Velankar et al. (2004), which was specifically devised for the situations in which the shoulder in G' is prominent and well-separated from any higher frequency relaxations. The G' expected from the components was first subtracted from the measured G' of the blend. The remainder, which may be regarded as the interfacial contribution to the G' , was fitted to a sum a few (up to 3) Maxwell modes:

$$G'(\omega) = \sum_{k=1}^n \frac{\omega^2 \exp(a_k + 2t_k)}{1 + \omega^2 \exp(2t_k)} \quad (17)$$

Fits were performed using the free gnuplot software as described previously (Velankar et al. 2004). A sample fit has been shown in Fig. 6, and additional examples have been shown previously (Velankar et al. 2004). In all cases, the Maxwell mode corresponding to the shoulder in G' was separated from any other modes by at least one decade in frequency. Thus, for all practical purposes, the shoulder can be captured by only one Maxwell mode. The corresponding relaxation time, multiplied by the shear rate prior to cessation of shear, yields the dimensionless relaxation time λ_{F1}^* . Equation 8 is then used to obtain the Ca.

References

- Graebling D, Muller R, Palierne JF (1993a) Linear viscoelastic behavior of some incompatible polymer blends in the melt. Interpretation of data with a model of emulsion of viscoelastic liquids. *Macromolecules* 26:320–329
- Graebling D, Muller R, Palierne JF (1993b) Linear viscoelasticity of incompatible polymer blends in the melt in relation with interfacial properties. *J De Physique Iv* 3:1525–1534
- Graebling D, Benkira A, Gallot Y, Muller R (1994) Dynamic viscoelastic behavior of polymer blends in the melt—experimental results for PDMS/POE-DO, PS/PMMA and PS/PEMA blends. *Eur Polymer J* 30:301–308
- Gramespacher H, Meissner J (1992) Melt elongation and recovery of polymer blends, morphology, and influence of interfacial tension. *J Rheol* 41:27–44
- Gramespacher H, Meissner J (1995) Reversal of recovery direction during creep recovery of polymer blends. *J Rheol* 39:151–160
- Jacobs U, Fahrlander M, Winterhalter J, Friedrich C (1999) Analysis of Palierne's emulsion model in the case of viscoelastic interfacial properties. *J Rheol* 43:1497–1509
- Kitade S, Ichikawa A, Imura N, Takahashi Y, Noda I (1997) Rheological properties and domain structures of immiscible polymer blends under steady and oscillatory shear flows. *J Rheol* 41:1039–1060
- Maffettone PL, Minale M (1998) Equation of change for ellipsoidal drops in viscous flow. *J Non-Newtonian Fluid Mech* 78:227–241
- Oldroyd JG (1953) The elastic and viscous properties of emulsions and suspensions. *Proc Roy Soc Lon A* 218:122–132
- Taylor GI (1934) The formation of emulsions in deformable fluids of flow. *Proc Roy Soc Lon A* 146:501–523
- Tucker CL, Moldenaers P (2002) Microstructural evolution in polymer blends. *Annu Rev Fluid Mech* 34:177–210
- Velankar S, Van Puyvelde P, Mewis J, Moldenaers P (2001) Effect of compatibilization on the breakup of polymeric drops in shear flow. *J Rheol* 45:1007–1019
- Velankar S, Van Puyvelde P, Mewis J, Moldenaers P (2004) Steady-shear rheological properties of model compatibilized blends. *J Rheol* 48:725–744
- Vinckier I, Mewis J, Moldenaers P (1996) Relationship between rheology and morphology of model blends in steady shear flow. *J Rheol* 40:613–632
- Vinckier I, Moldenaers P, Mewis J (1999) Elastic Recovery of immiscible blends I. Analysis after steady state shear flow. *Rheol Acta* 38:65–72